Coexisting periodic attractors in injection locked diode lasers

A. Gavrielides, V. Kovanis and P.M. Varangis
Nonlinear Optics Center, Phillips Laboratory,
Kirtland AFB, NM 87117-5776

T. Erneux and G. Lythe[*]
Université Libre de Bruxelles, Optique Nonlinéaire Théorique,
Campus Plaine, C.P. 231, 1050 Bruxelles, Belgium

Abstract

We present experimental evidence of coexisting periodic attractors in a semiconductor laser subject to external optical injection. The coexisting attractors appear after the semiconductor laser has undergone a Hopf bifurcation from the locked steady state. We consider the single mode rate equations and derive a third order differential equation for the phase of the laser field. We then analyze the bifurcation diagram of the time periodic states in terms of the frequency detuning and the injection rate and show the existence of multiple periodic attractors.

---

[*]Present Address: Center for Nonlinear Studies, Los Alamos National Laboratory, Los Alamos, NM 87545

1 Introduction

Semiconductor lasers have a wide range of applications because they are of relatively small size, they can be massively produced at low cost, and they are easy to operate. Applications of semiconductor lasers appear in many areas such as optical communication and high speed modulation and detection. Despite their successful technology, semiconductor lasers are quite sensitive to any external perturbation which may destabilize their normal output. A small amount of optical feedback resulting from the reflection from an optical disk or from the end of an optical fiber is sufficient to generate pulsating instabilities. These oscillations are typically accompanied by higher intensity of frequency noise and affect the normal efficiency of the laser.

Systematic experimental studies of semiconductor lasers, in particular long time series analysis of the intensity are not available because the time scale of the intensity pulsations is typically in the picosecond regime. Fourier spectra measurements show a gradual increase of oscillatory instabilities as parameters are changed but do not reveal what are the bifurcation mechanisms. Most of the progress on our understanding of these bifurcations comes from extensive numerical studies of simple models and their comparison to the experimentally obtained Fourier spectra. Specifically, these are the Lang and Kobayashi equations [1] for a single mode laser subject to optical feedback [2], the equations for two coupled lasers [3], and the equations for a laser subject to external optical injection [4]. The latter is presumably the simplest system which allows a study of instabilities induced by an external perturbation.

The rate equations in normalized form for this system consist of two equations for the complex electrical field E and the excess carrier number N given by:

$$E' = (1 - ib)NE + \eta E_i, \tag{1}$$

$$TN' = P - N - P(1 + 2N)|E|^2 \tag{2}$$

where prime means differentiation with respect to time t measured in units of the photon lifetime τ_p. The term $\eta E_i = \eta \exp(-i\Omega t)$ models the electrical field of the injected signal which is controlled by changing either its amplitude η or its detuning Ω. The equations are the same for a laser subject to optical feedback or

for each laser in arrays of coupled lasers. They differ only by the last term in Eq. (1). The fixed parameters b, T and P are defined as follows: b is the linewidth enhancement factor ($b = 3 - 6$) which measures the amount of amplitude-phase coupling; $T \equiv \tau_s/\tau_p$ is the ratio of the carrier and photon lifetimes ($T \simeq 10^3$) and P is the dimensionless pumping current above threshold ($|P| < 1$). A series of recent experiments have explored a large variety of dynamical instabilities at high injection levels and have been simulated successfully by using Eqs. (1) and (2). The comparison is particularly remarkable knowing the high simplicity of these equations. They correctly describe the observed period doubling cascade to chaos [5], the period 2 bubbles [6], as well as the details of the experimental map of all the instability regions in the detuning versus injection amplitude parameter space [7].

Of particular interest are the conditions for locking which corresponds to a steady phase of the laser field and occurs if the detuning is sufficiently low. This phenomenon is best analyzed by introducing $E = R \exp[i(\Phi - \Omega t)]$ into Eqs. (1) and (2) and by studying the conditions for a steady phase Φ. If the injection level is very weak, it is reasonable to assume that the laser amplitude and the carrier number will approach their steady state values in the absence of injection (i.e., $R \simeq 1$ and $N \simeq 0$) and that the long time behavior of the laser is first described by the phase Φ. From the equations for R, Φ and N, it is then straightforward to find that Φ satisfies Adler equation

$$\Phi' = \Omega - \eta \sin(\Phi). \qquad (3)$$

Locking now implies the condition $|\Omega| \leq \eta$. In addition to locking, Eq. (3) has been used to investigate the case of an unbounded phase (i.e., if $|\Omega| > \eta$). Specifically, if $\eta << \Omega$, $\Phi \simeq \Omega t$ which implies a small amplitude periodic modulation of the laser amplitude equation i.e., $R' = RN + \eta \cos(\Phi) \simeq RN + \eta \cos(\Omega t)$.

This case has been studied analytically [8] and is called four wave mixing because of the typical Fourier spectra. However, the practical interest of (3) is limited by the fact that T is a large parameter. The effect of T large can be first analyzed from Eqs. (1) and (2) with $\eta = 0$. We find that small perturbations from the steady state $(R, N) = (1, 0)$ slowly decays on an $O(T)$ time interval with rapid oscillations characterized by period $2\pi/\omega = O(\sqrt{T})$ where $\omega \equiv \sqrt{2P/T}$ is the laser relaxation oscillations frequency. We take this property into account by introducing the new time $s \equiv \omega t$ and by reformulating Eqs. (1) and (2) in terms of normalized deviations from the steady state, namely, $x \equiv N\omega^{-1}$ and $y \equiv R - 1$. By then investigating the limit $\omega \to 0$ (equivalently, T large) of the

3

resulting equations for x, y and Φ, we reobtain (3) provided that $\Omega = O(\eta)$ and

$$\eta \leq \omega^2 = O(T^{-1}). \tag{4}$$

Thus, (3) is only valid for relatively low injection. It explains the locking phenomenon and the entrainement of the laser in the four wave mixing regime but cannot lead to the multiple instabilities observed experimentally and numerically.

In particular, we show in Figures 1a and 1b experimentally obtained spectra of a semiconductor laser subject to injection operating at very low detunings between the frequencies of the slave and master laser. The spectra were taken at constant injection and detuning. They show the characteristic sidebands at the relaxation oscillations frequency indicating that a Hopf bifurcation has taken place from the locked steady state. The laser exhibited the two spectra at various times. The transition from one spectrum to another was abrupt strongly suggesting that the laser was visiting two different periodic states assisted by the intrinsic noise in the system. This implies that another stable periodic state may coexist with the Hopf bifurcation periodic state for the same values of the parameters. Figures 2a and 2b show spectra obtained from solving numerically the single mode rate equations (1) and (2). The parameters used for these simulations were $T = 1000$, $b = 4$, $P = 1.0$, $\eta = 0.002$ and $\Omega/\omega = 0.1$. These values of the parameters are of the same order as the values that have been used before by a number of authors to model the HLP-1400 semiconductor lasers (emitting at 830 nm). These lasers were also used in this set of experiments [9]. Gain saturation, known to shift bifurcation points, did not alter our conclusions, producing only minor modifications of the spectra. Figure 3 shows the bifurcation diagram of the periodic states. In addition to the periodic states emerging from the Hopf bifurcation, there is an isolated branch of periodic states emerging from a limit point. The spectra shown in Figures 2a and 2b were computed at the points denoted by A and B in Figure 3, respectively. They compare well with the experimental spectra shown in Figures 1a and 1b.

Bifurcation diagrams exhibiting coexisting bifurcation and isolated branches of periodic attractors are not common for nonlinear bifurcation problems. Similar diagrams have been found numerically for the laser subject to optical feedback [17] suggesting that the emergence of coexisting branches of periodic attractors is a general feature of semiconductor laser instabilities. This motivates analytical studies of the laser rate equations which we describe in the next two sections. In Section 2, we formulate a third order phase equation which is a major simplification of the original laser equations. In Section 3, we analyze this equation and determine approximations for the steady and time-periodic solutions.

2 Formulation

Intensive numerical studies of the first period doubling bifurcation in the simplest case of zero detuning [10] showed that the linewidth enhancement factor plays a key role in the problem. Its relatively large value compared to the other constants in the problem explains why the intensity oscillations are nearly harmonic in time and how a strong coupling between phase and laser amplitude is possible. This can be demonstrated by a new asymptotic analysis of the original equations using b as the order parameter. To this end, we first introduce the decomposition $E = R \exp[i(\Phi - \Omega t)]$ into Eqs. (1) and (2) and reformulate the resulting three equations in terms of new variables defined by

$$s \equiv \omega t, \mathrm{x} \equiv \mathrm{N}b\omega^{-1} \mathrm{and} \mathrm{y} \equiv \mathrm{b}(\mathrm{R} - 1). \tag{5}$$

In (5), time is scaled by the relaxation oscillations frequency $\omega \equiv \sqrt{2P/T}$ and x, y represent deviations from the zero injection steady state solution $(R, N) = (1, 0)$. The resulting equations for x, y and Φ are then analyzed for large b assuming $\omega = O(b^{-1})$ (see Appendix). The reduced problem - accurate to $O(b^{-1})$ - is described in terms of the phase Φ and is given by (35), or equivalently,

$$\begin{aligned}
\Phi''' + (\xi - 2b^{-1}\Delta)\Phi'' + \Phi' - \Delta - \Lambda\cos(\Phi) \\
= b^{-1}[\Lambda\sin(\Phi)\Phi'^2 - \Lambda\sin(\Phi) - 2\Phi'\Phi'']
\end{aligned} \tag{6}$$

where prime now means differentiation with respect to time s. The parameters Λ, Δ and ξ are defined by

$$\Lambda \equiv \frac{\eta b}{\omega}, \Delta \equiv \frac{\Omega}{\omega} \text{ and } \xi \equiv \omega\frac{1 + 2\mathrm{P}}{2\mathrm{P}} \tag{7}$$

and correspond to the normalized injection, normalized detuning and laser damping parameters, respectively. The leading order problem as $b^{-1} \to 0$ (ω small but fixed) is

$$\Phi''' + \xi\Phi'' + \Phi - \Delta - \Lambda\cos(\Phi) = 0 \tag{8}$$

and was previously examined for the case $\Delta = 0$ (zero detuning) [10]. In particular, its validity has been carefully investigated by comparing the numerical bifurcation diagrams obtained from Eqs. (1) and (2) and from Eq. (8). The two bifurcation diagrams have been compared for various ranges of values of the parameters T and b including the experimental parameters estimated in [5], [6] and

[7]. The agreement between exact and approximate diagrams is excellent provided that the injection level is not too large (i.e., Λ must be $O(1)$ or smaller). For the case $\Delta \neq 0$, a direct comparison between experimental data and solutions of Eq. (8) has been undertaken if Δ is close to 2 and in the four wave mixing region. If $\Delta \simeq 2$, the laser exhibits two period doubling bifurcations which are not observed for other values of Δ and motivated the interest for this particular case. The optical spectra have been obtained for Δ below and above 2 which allow us to study both the sudden transition to subharmonic resonance and the progressive shift of the frequencies [11].

In this paper, we investigate Eq. (6). The steady states and their linear stability properties are easily determined for small b^{-1} and $\omega = O(b^{-1})$. We find that the steady states emerge from limit points located at

$$\Lambda = \Delta \tag{9}$$

and that they may change stability at Hopf bifurcation points located at

$$\Lambda = \sqrt{\Delta^2 + (\xi - 2b^{-1}\Delta)^2 + O(b^{-2})}. \tag{10}$$

From (9) and (10), we note that a limit point and a Hopf bifurcation point may coalesce if $\Delta = \Delta_c$ and $\Lambda = \Lambda_c$ where

$$\Delta_c \simeq \xi b/2 \text{and} \Lambda_c = \Delta_c. \tag{11}$$

This degenerate Hopf bifurcation point was already noticed from the exact linear stability analysis [12]. It corresponds to a zero eigenvalue and a pair of imaginary eigenvalues of the linearized theory and may lead to a secondary bifurcation to quasiperiodic oscillations [13].

3 Bifurcation equations

The phase equation (8) is a major simplification of the original laser equations. It models the laser problem as a weakly damped harmonic oscillator strongly driven by the phase of the laser field but it is still too complicated for exact solutions. In this section, we determine an asymptotic solution of Eq. (6) valid for small b^{-1}, Λ, Δ and ξ by the method of multiple scales [15]. To this end, we expand the parameters as

$$\Lambda = b^{-1}(\lambda + b^{-1}\lambda_1 + ...), \qquad \Delta = b^{-1}(\delta + b^{-1}\delta_1 + ...),$$
$$\xi \equiv \omega\frac{1+2P}{2P} = b^{-1}(\sigma + b^{-1}\sigma_1 + ...) \tag{12}$$

and seek a solution of the form

$$\Phi(s, \tau, b^{-1}) = \Phi_0(s, \tau) + b^{-1}\Phi_1(s, \tau) + ... \tag{13}$$

where $\tau \equiv b^{-1}s$ is defined as a slow time variable. The fact that the solution depends on two independent time variables implies the chain rule $\Phi' = \Phi_s + b^{-1}\Phi_\tau$ where subscripts mean partial derivatives.

Inserting (12) and (13) into Eq. (6) and equating to zero the coefficients of each power of b^{-1} leads to a sequence of linear problems for the coefficients $\Phi_0, \Phi_1, ...$ Solving the equation for Φ_0 gives

$$\Phi = A\sin(s + v) + B + O(b^{-1}) \tag{14}$$

where the amplitudes A and B and the phase v are functions of the slow time τ. We obtain equations for A, B and v by considering the problem for Φ_1 and by applying solvability conditions [15]. The equation for v is simply $v' = 0$ which means that v is equal to its initial value. The equations for A and B are given by

$$A' = -\frac{1}{2}\sigma A + \lambda\sin(B)J_1(A) \tag{15}$$

$$B' = \delta + \lambda\cos(B)J_0(A) \tag{16}$$

where $J_0(A)$ and $J_1(A)$ are Bessel functions which come from the expansion of $\cos(\Phi)$ in Fourier series. Note that the modified phase equation (6) and the leading order phase equation (8) lead to the same amplitude equations at this order of the analysis. Eqs.(15) and (16) admit steady state solutions which we analyze in detail. The simplest solution is given by

$$(1)A = 0 \quad \text{and} \quad \Lambda = -\Delta\cos^{-1}(B) > 0 \tag{17}$$

and corresponds to the steady state of the original equation (8). The second steady state solution of Eqs.(15) and (16) is characterized by the fact that $A \neq 0$ and corresponds to time-periodic solutions of Eq. (8). It is instructive to examine this

7

solution for $\Delta = 0$ first. From Eq. (16) with $B' = \delta = 0$, we find two possibilities. The first family of solutions verifies the condition $\cos(B) = 0$ and is described by

$$(2a)\mathrm{B} = \pm\frac{\pi}{2} \quad \text{and} \quad \Lambda = \pm\frac{\xi\mathrm{A}}{2\mathrm{J}_1(\mathrm{A})} > 0. \tag{18}$$

From (18), we determine a Hopf bifurcation branch emerging from Solution (1) at $(\Lambda, A, B) = (\Lambda^H, 0, \frac{\pi}{2})$. Λ^H is found from (18) by taking the limit $A \to 0$. We obtain

$$\Lambda^H = \xi \tag{19}$$

which is correctly matching (10) if $\Delta = 0$. But Eq. (18) describes other branches of solutions. These branches of solutions are isolated and emerge from limit points that satisfy the condition $\Lambda'(A) = 0$. Using the second expression in (18), we find that these limit points are located at $(\Lambda, A, B) = (\Lambda^L, A^L, \pm\frac{\pi}{2})$ where A^L and Λ^L satisfies the condition

$$J_2(A^L) = 0 \quad \text{and} \quad \Lambda^L = \pm\frac{\xi A^L}{2J_1(A^L)} > 0. \tag{20}$$

The second family of solutions characterized by an $A \neq 0$ verifies the condition $J_0(A) = 0$ and is described by

$$(2b)\mathrm{J}_0(\mathrm{A}) = 0 \quad \text{and} \quad \Lambda = \frac{\xi\mathrm{A}}{2\sin(\mathrm{B})\mathrm{J}_1(\mathrm{A})} > 0. \tag{21}$$

This solution emerges from Solution $(2a)$ at the pitchfork bifurcation point located at $(\Lambda, A, B) = (\Lambda^{PF}, A^{PF}, \pm\frac{\pi}{2})$ where

$$J_0(A^{PF}) = 0 \quad \text{and} \quad \Lambda^{PF} = \pm\frac{\xi A^{PF}}{2J_1(A^{PF})} > 0. \tag{22}$$

In the case of nonzero detuning ($\Delta \neq 0$), we find that all $A \neq 0$ steady state solutions of Eqs. (15) and (16) are described by (in implicit form)

$$\Lambda = \left[\left(\frac{\Delta}{\mathrm{J}_0(\mathrm{A})}\right)^2 + \left(\frac{\xi\mathrm{A}}{2\mathrm{J}_1(\mathrm{A})}\right)^2\right]^{1/2} \quad \text{and} \quad \mathrm{B} = \arccos\left(-\frac{\Delta}{\Lambda\mathrm{J}_0(\mathrm{A})}\right). \tag{23}$$

Eq. (23) reveals several branches of solutions which converge to Solution $(2a)$ and Solution $(2b)$ as $\Delta \to 0$. In Figure 4, we show the bifurcation diagram

of the solutions of Eqs. (15) and (16) in terms of A vs Λ. The solid and dotted lines correspond to $\Delta = 0$ and $\Delta = 0.01$, respectively. All stable and unstable branches of solutions have been drawn. Note the coexistence of multiple branches of solutions emerging from limit points. If $\Delta = 0$, these limits points correspond to simple roots of Bessel functions (see Eq.(20) and Eq.(22)).

The numerical bifurcation diagram of the stable solutions of Eq.(8) with $\Delta = 0$ is shown in Figure 5. Figures 5a and 5b represent the extrema of the phase Φ and the intensity variable $y \equiv b(R-1)$, respectively. The pitchfork bifurcation at (22) leading to two distinct branches of B is clearly identified in Figure 5a. These two branches are not seen in Figure 5b because $y = \Phi'' \simeq -A\sin(s + v)$ from (33) and is independent of B, in first approximation (equivalently, the extrema of y are equal to $\pm A$, in first approximation). The figure shows one isolated branch of stable periodic states that coexist with the bifurcation branch. The bifurcation at $\Lambda \sim 0.65$ is a period doubling bifurcation which is not predicted by Eqs. (15) and (16) and which requires a different analysis [10].

The unfolding of the $\Delta = 0$ bifurcation diagram as Δ is progressively increased is illustrated by the dotted lines in Figure 4. In Figure 6, we represent the extrema of y for all stable solutions determined numerically from (8) with $\Delta = 0.01$. The agreement between numerical and analytical solutions is excellent (compare Figure 4 and Figure 6).

The amplitude equations (15) and (16) admit a third family of solution if $|\Delta/\Lambda| > 1$. These solutions correspond to $A = 0$ and an unbounded B satisfying Adler's equation, $B' = \Delta + \Lambda\cos(B)$. We have verified that all solutions of this equations are linearly stable with respect to small perturbations in A. Φ is then unbounded but Φ' is bounded (equivalently, $x \simeq \Delta - \Phi'$ and $y \simeq \Phi''$ are bounded). This solution is the four wave solution for small Λ and $\Delta = O(\Lambda)$.

In summary, our analysis of the phase equation (8) has revealed several branches of periodic solutions which allows the coexistence of different periodic states oscillating harmonically in time with similar periods but exhibiting differing amplitudes. Coexisting periodic states oscillating harmonically in time were also observed for the laser subject to optical feedback [17]. Both for the laser subject to injection and the laser subject to optical feedback, it is the strong phase/amplitude coupling parameterized by the linewidth enhancement factor b that is the main mechanism leading to this multiplicity of attractors.

Note that these periodic states appear as isolated branches of solutions. The traditional way to determine the bifurcation diagram of the long time regimes is to follow each branch of solutions as a parameter is progressively changed and carefully determine changes of stabilities between each states. This method is

used both experimentally and numerically but will fail to find isolated branches of solutions.

Isolated branches of solutions have been found numerically and experimentally for periodically modulated lasers [16]. These branches correspond to different resonances and coexisting periodic states admit different periods. In the case of a semiconductor laser subject to feedback, two periodic coexisting attractors were observed experimentally and computed numerically by Mork *et al* [2]. More recently, De Jagher *et al* [18] reported two coexististing periodic solutions which may result from the emergence of isolated branches of solutions as described in this paper. From a practical point of view, it could be interesting to force the semiconductor laser to operate at these higher intensity states and investigate possible application in communications or in logic gates.

4   Discussion

We have shown analytically that the single mode equations admit multiple periodic states emerging from limit points in addition to periodic solutions that appear as the result of a Hopf bifurcation from the steady state. In general, the spectra of two of the limit cycles might appear very similar if they are taken at an injection level at which the amplitude saturates and approaches constant values. However for low injection levels and away from saturation the spectra can exhibit dramatic differences. This is clearly demonstrated by the computed spectra shown in Figure 2. In particular small perturbations in the phase of the field can induce dramatic changes in the optical spectra. This is precisely the reason that the multiple instabilities exhibited by the phase of the field can be clearly observed in the spectra. Such effects include center line suppression, in which the center line of the laser is almost devoid of energy most of which is carried by the sidebands at the relaxation frequency. This is a typical feature of a laser with a large value of the linewidth enhancement factor.

The effect of gain saturation can also be incorporated in the context of the phase equation formalism. Its main contribution is to shift Hopf bifurcation and limit points but it would not modify the qualitative properties of the bifurcation diagram.

We note that the period doubling bifurcation point can also be captured analytically from Eq. (8) by seeking a solution of the form $\Phi \simeq A \sin(s) + D \cos(s/2)$. If $\Delta = 0$, we obtain

$$\Lambda_{PD} \simeq 0.62 \tag{24}$$

which compares well with the prediction of Figure 5a. If $\Delta \neq 0$, we find that the period doubling bifurcation point $\Lambda_{PD}(\Delta)$ is - in parametric form - given by

$$\Lambda_{PD} = \frac{0.32}{J_1(A)}, \Delta = \pm 0.32\frac{J_0(A)}{J_1(A)} \tag{25}$$

where $O(\xi)$ terms have been neglected.

The existence of sustained quasiperiodic oscillations has been suggested numerically but require a more detailed bifurcation analysis. Furthermore, experimental evidence of quasiperiodic oscillations is still lacking. This is partly because the laser is not stable at this injection region and frequently mode hops to a different cavity line. In addition the transition to the quasiperiodic behavior is a weak phenomenon and it is difficult to extract the signal from background noise.

In conclusion by taking advantage of the two large parameters T and b that are naturally present in semiconductor lasers, we are able to reduce the original single mode rate equations into a third order pendulum type phase equation. This equation then allowed us to predict isolated branching of solutions which can not be anticipated using traditional continuation methods.

5   Appendix: derivation of the phase equation

We first introduce the decomposition $E = R\exp[i(\Phi - \Omega t)]$ into Eqs. (1) and (2) and obtain the following three equations for A, Φ and N

$$R' = NR + \eta\cos(\Phi), \tag{26}$$

$$\Phi' = \Omega - bN - \frac{\eta}{R}\sin(\Phi), \tag{27}$$

$$TN' = P - N - P(1 + 2N)R^2. \tag{28}$$

In Eqs. (26)-(28), T is a large parameter that multiplies N'. We remove this source of singularity by introducing the new variables s, x and y defined by (5). Eqs. (26)-(28) then become

$$y' = x(1 + b^{-1}y) + \Lambda\cos(\Phi), \tag{29}$$

$$\Phi' = \Delta - x - \Lambda b^{-1} \frac{\sin(\Phi)}{1 + b^{-1}y}, \tag{30}$$

$$x' = -\xi x - y - 2\omega b^{-1}xy - \frac{1}{2}b^{-1}y^2 - \omega b^{-2}xy^2. \tag{31}$$

where ξ, Λ and Δ are dimensionless parameters defined by (7). Note that ξ is proportional to ω and that ω is an $O(T^{-1/2})$ small quantity. Our problem depends on two small parameters, namely b^{-1} and ω. The derivation of our simplified problem will be based on the limit b^{-1} assuming $\omega = O(b^{-1})$.

¿From Eqs. (30), we find x as a function Φ

$$x = \Delta - \Phi' - \Lambda b^{-1}\sin(\Phi) + O(b^{-2}) \tag{32}$$

and from Eq.(31), using (32), we find y as

$$y = -\xi x - x' + O(b^{-1}) = \Phi'' + O(b^{-1}, \omega). \tag{33}$$

(Note: the $O(b^{-1})$ correction term in (32) is needed but the $O(b^{-1})$ and $O(\omega)$ correction terms in (33) are not). In order to derive an equation for Φ only, we first differentiate Eq. (31) once and eliminate y' using (29). We find

$$x'' = -\xi x' - \left[x(1 + b^{-1}y) + \Lambda\cos(\Phi)\right] - b^{-1}y\left(x + \Lambda\cos(\Phi)\right) + O(b^{-2}, b^{-1}\omega). \tag{34}$$

We next use (32) and (33) and eliminate x and y in (34). This leads to the following third order equation for Φ given by

$$\begin{aligned}\Phi''' + \Phi' - \Delta - \Lambda\cos(\Phi) \\ +b^{-1}\left[\Phi''\left(b\xi - 2(\Delta - \Phi')\right) + \Lambda\sin(\Phi) - \Lambda\sin(\Phi)\Phi'^2\right] + O(b^{-2}, b^{-1}\omega)\end{aligned} \tag{35}$$

where $b\xi = O(b\omega)$ is $O(1)$.

6 Acknowledgments

References

[1] R. Lang and K. Kobayashi, IEEE J. Quantum Electron. **16**, 347 (1980).

[2] J. Mork, J. Mark and B. Tromborg, Phys. Rev. Lett. **65**, 1999 (1990).

[3] H.G. Winful and S.S. Wang, Appl. Phys. Lett. **53**, 1894 (1988).

[4] R. Lang, IEEE J. Quantum Electron. **18**, 976 (1982).

[5] T.B. Simpson, J.M. Liu, A. Gavrielides, V. Kovanis, and P.M. Alsing, Appl. Phys. Lett. **64**, 3539 (1994).

[6] T.B. Simpson, J.M. Liu, A. Gavrielides, V. Kovanis, and P.M. Alsing, Phys. Rev. A **51**, 4181 (1995).

[7] V. Kovanis, A. Gavrielides, T.B. Simpson, J.M. Liu, Appl. Phys. Lett. **67**, 2780 (1995).

[8] D. Lenstra, G.H.M. van Tartwijk, W.A. van der Graaf, and P.C. de Jagher, SPIE **2039**, 11 (1993).

[9] H. Li, J. Ye and J.G. McInerney, IEEE J. Quantum. Electron. **29**, 2421 (1993).

[10] T. Erneux, V. Kovanis, A. Gavrielides and P. M. Alsing, Phys. Rev. A **53**, 4372 (1996).

[11] A.Gavrielides, V. Kovanis, P. M. Varangis, T. Erneux and T. Simpson, SPIE **3693**, 654 (1996).

[12] A. Gavrielides, V. Kovanis and T. Erneux, "Stability boundaries for a semiconductor laser subject to optical injection" Optics Communications 1997.

[13] J. Guckenheimer and P. Holmes, *Nonlinear Oscillations, Dynamical Systems, and Bifurcations of vector Fields,* Applied Mathematical Sciences 42, Springer-Verlag (1983).

[14] E. K. Lee, H. S. Pang, J. D. Park and H. Lee, Phys. Rev. A **47**, 736 (1993).

[15] J. Kevorkian and J. D. Cole, *Perturbation Methods in Applied Mathematics*, Applied Mathematical Sciences 34, Springer Verlag (1981).

[16] D.Dangoisse, P. Glorieux and D. Hennequin, Phys. Rev. Lett. **57**, 2657, (1986); Phys. Rev. A **36**, 4775 (1992).

[17] P.M. Alsing, V. Kovanis, A. Gavrielides and T. Erneux , Phys. Rev. A **53**, 4429 (1995).

[18] P. C. De Jagher, W. A. van der Graaf and D. Lenstra, Quantum Semiclass. Opt. **8**, 805 (1996).

Figure captions

Figure 1 Experimentally obtained optical spectra of the laser subject to injection in the neighborhood of the Hopf bifurcation. f_r is defined as the free running relaxation oscillation frequency, $f_r = \frac{1}{2\pi}\sqrt{2P/T}$.

Figure 2 Numerically computed optical spectra from the single mode rate equations (1) and (2) for $T = 1000$, $b = 4$, $P = 1.0$, $\eta = 0.002$ and $\Omega/\omega = 0.1$. The zero of the frequency scale denotes the frequency of the master laser.

Figure 3 Bifurcation diagram of the extrema of the deviation of the field from steady state as a function of injection. The solutions are computed from the rate equations (1) and (2) using the same values of the parameters as in Figure 2. The points denoted by A and B indicate where the spectra in Figures 2a and 2b were numerically computed.

Figure 4 Bifurcation diagram of the amplitude A of the periodic solution versus Λ constructed form the analytic solutions of the phase equation for $T = 1000$, $b = 10$, $P = 0.5$. Solid lines are for $\Delta = 0$ and dotted lines for $\Delta = 0.01$.

Figure 5 Bifurcation diagram obtained numerically from the phase equation (8) for $T = 1000$, $b = 10$, $P = 0.5$, and zero detuning. **(a)** shows the extrema of the phase Φ versus injection Λ; **(b)**. shows the extrema of the field versus injection.

Figure 6 Bifurcation diagram obtained numerically from the phase equation (8) for $T = 1000$, $b = 10$, $P = 0.5$, and $\Delta = 0.01$.
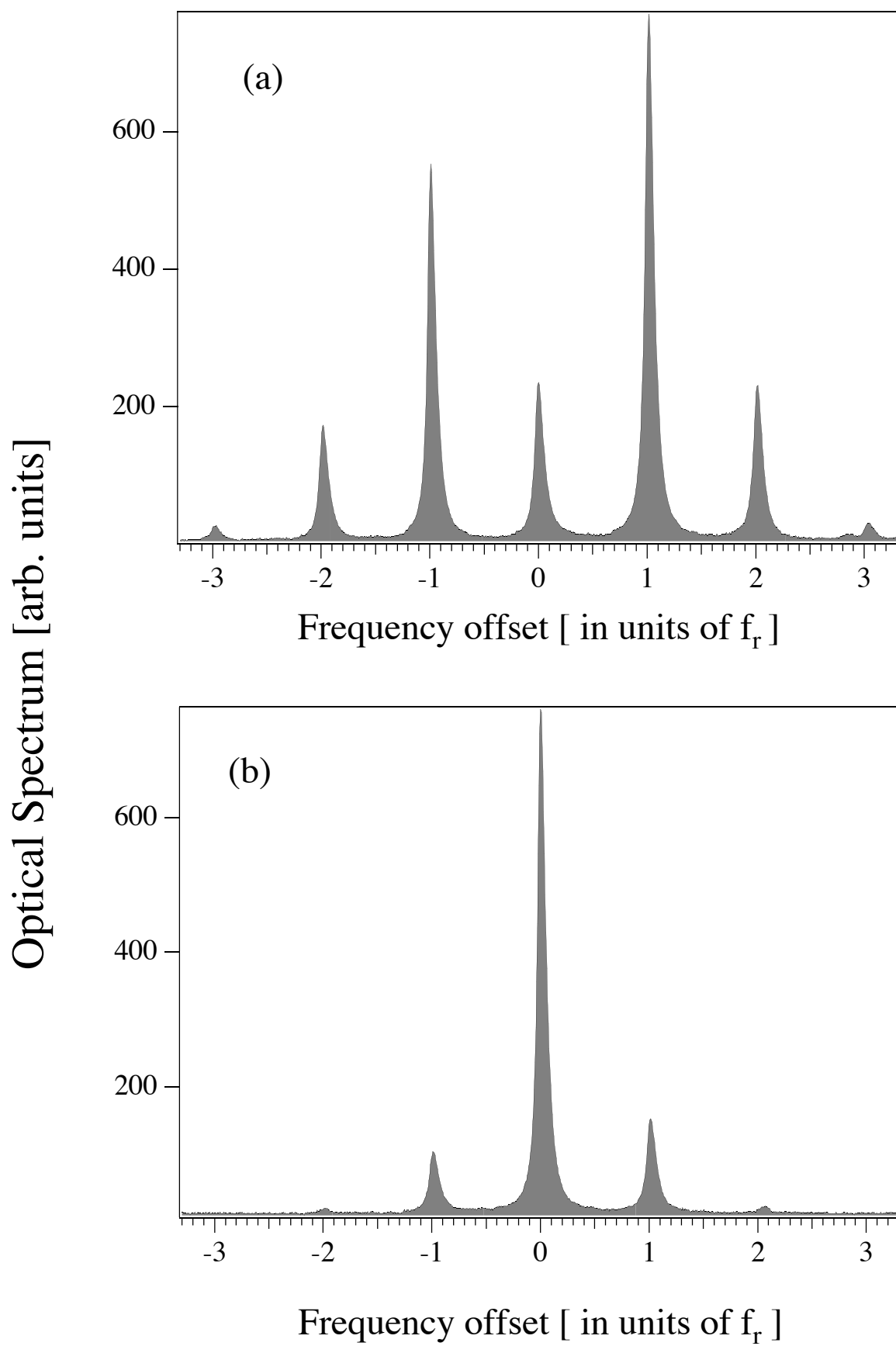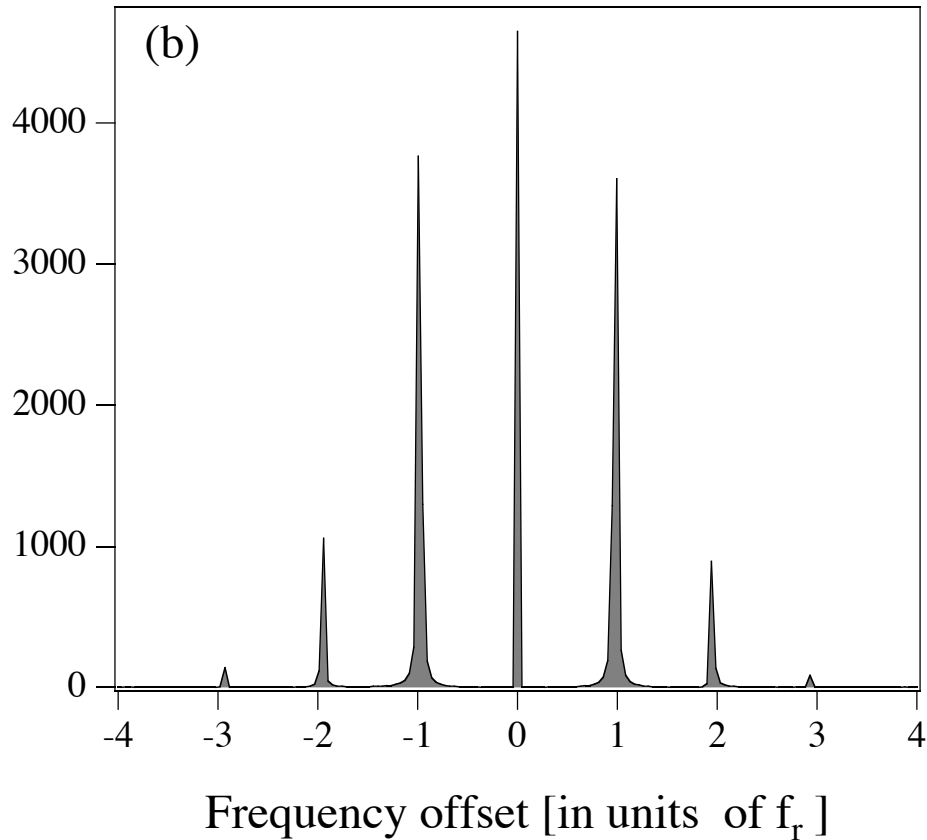
(a)

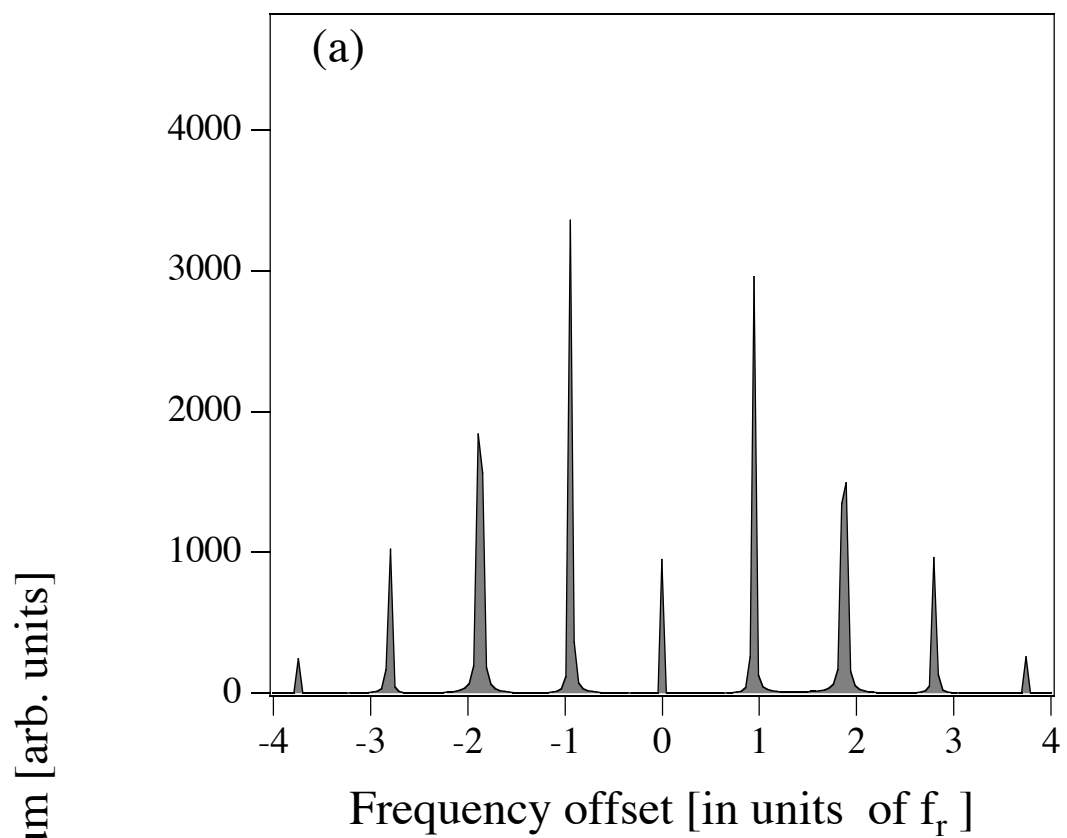Frequency offset [in units of f_r]

(b)

Frequency offset [in units of f_r]

Optical Spectrum [arb. units]

Figure 1

Figure 2

Extrema of y

A

B

0.8
0.6
0.4
0.2
0.0
-0.2
-0.4
-0.6
-0.8

1   2   3   4   5x10

η

(a)

Extrema of the phase

Λ

(b)

Extrema of y

Λ

(a)

Extrema of the phase

(b)

Extrema of y

Λ